

A grayscale photograph of a complex cryogenic heat exchanger system, featuring various pipes, valves, and a large cylindrical vessel. The image is semi-transparent, serving as a background for the title text.

Influence on the performance of cryogenic counter-flow heat exchangers due to longitudinal conduction, heat in-leak and property variations

Qingfeng Jiang

**Institute of Plasma Physics, Chinese Academy of Sciences
University of Science and Technology of China, Hefei, China**

12 July, 2017

A grayscale photograph of a wide river or lake with a line of trees and a path on the right side, serving as a background for the date.

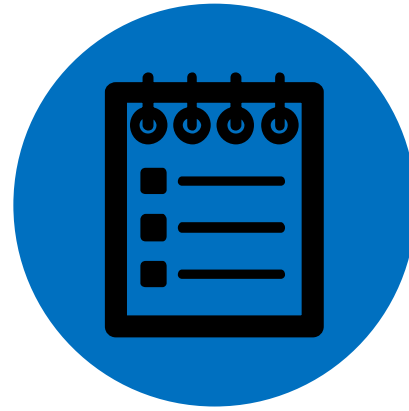
Outline



Introduction



Methodology

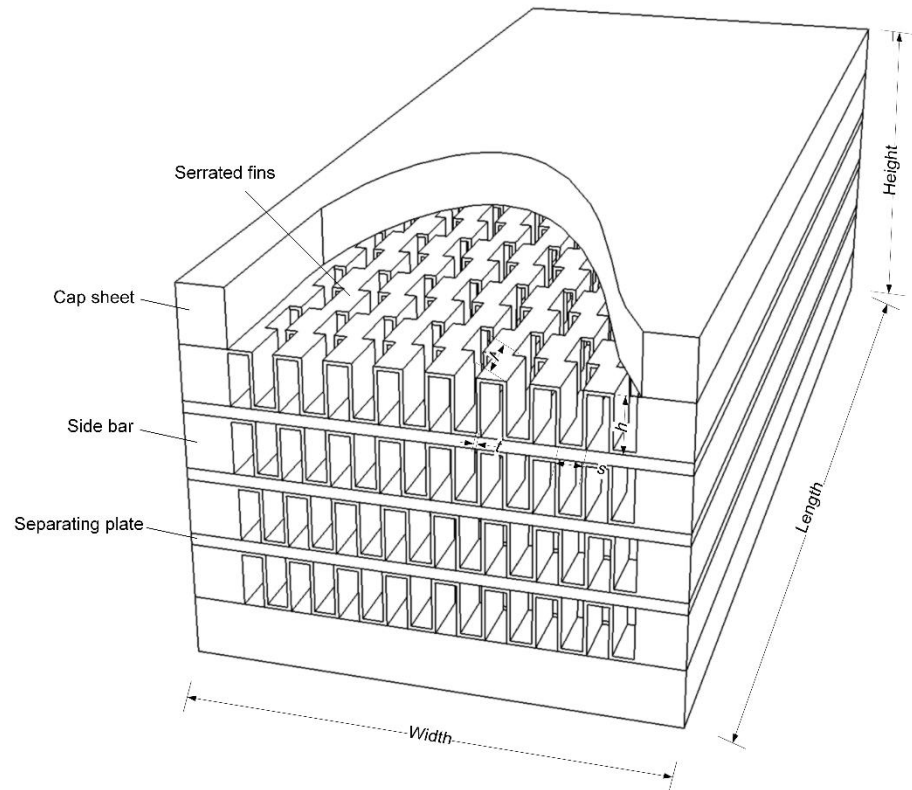


**Results and
discussions**

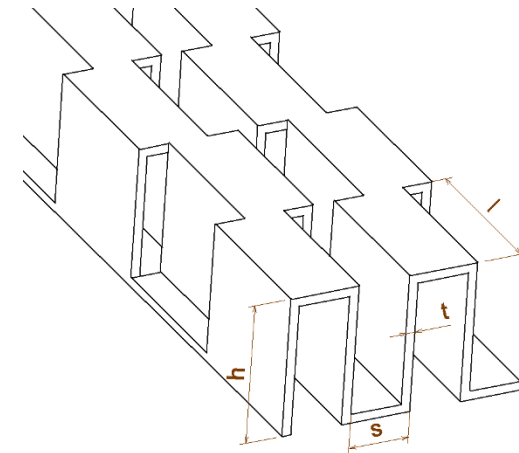


Summaries

Plate-fin heat exchangers (PFHEs)



The schematic of a multi-channel PFHE core



The diagram of offset strip fins



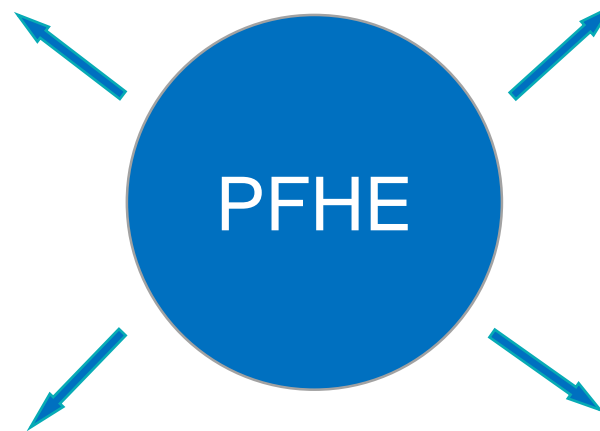
Aerospace



Automobile



Cryogenic industries



Air separation plants, etc.

1. Introduction

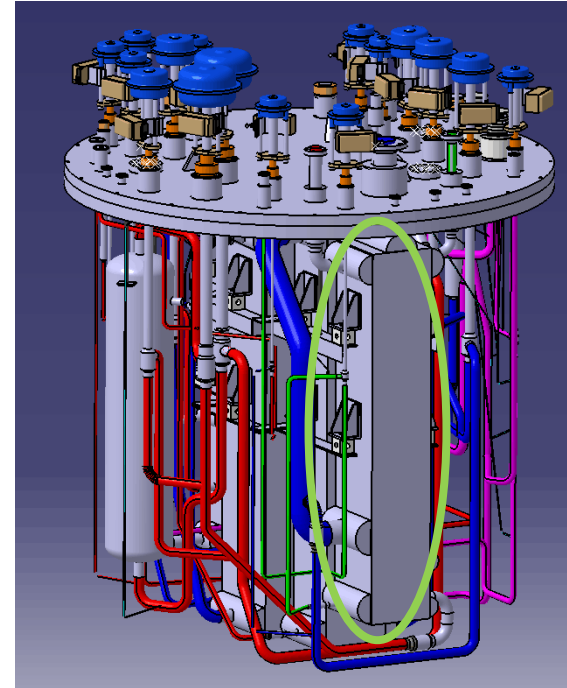
Helium liquefiers/refrigerators



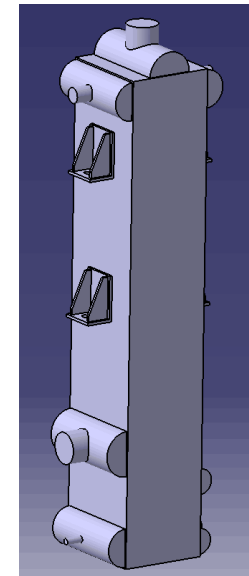
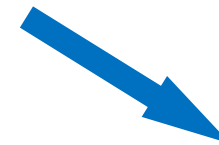
EAST tokamak



EAST helium refrigerator



Cold box



PFHE

1. Introduction

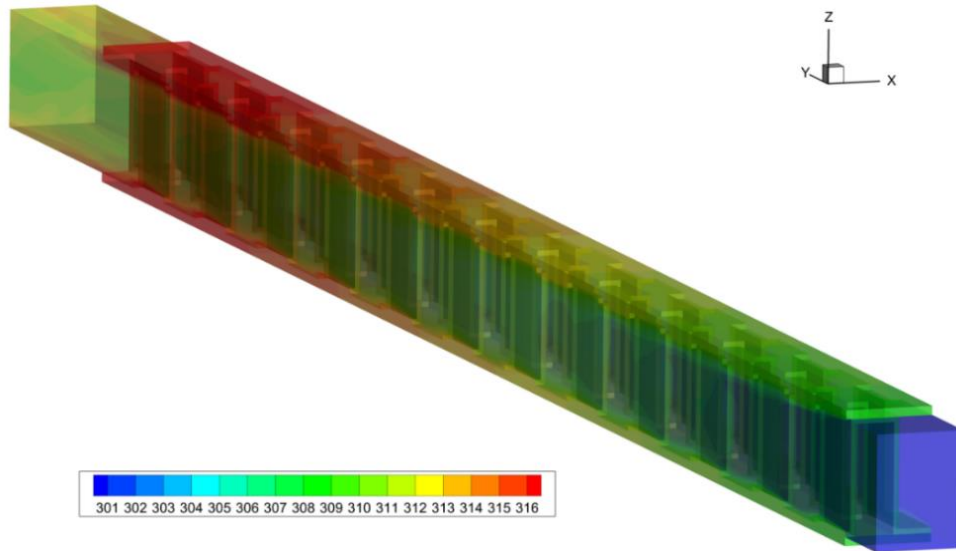
Table 1. Geometry of the heat exchanger (mm)

Core dimensions	Stream number	Fin type	Fin height	Fin space	Fin thickness	Interrupted length
350 × 1200 × 598	A	Serrated	4.7	2	0.3	3
	B	Serrated	9.5	1.4	0.2	3
	C	Serrated	9.5	1.4	0.2	3
	D	Serrated	9.5	1.4	0.2	3

1. Introduction

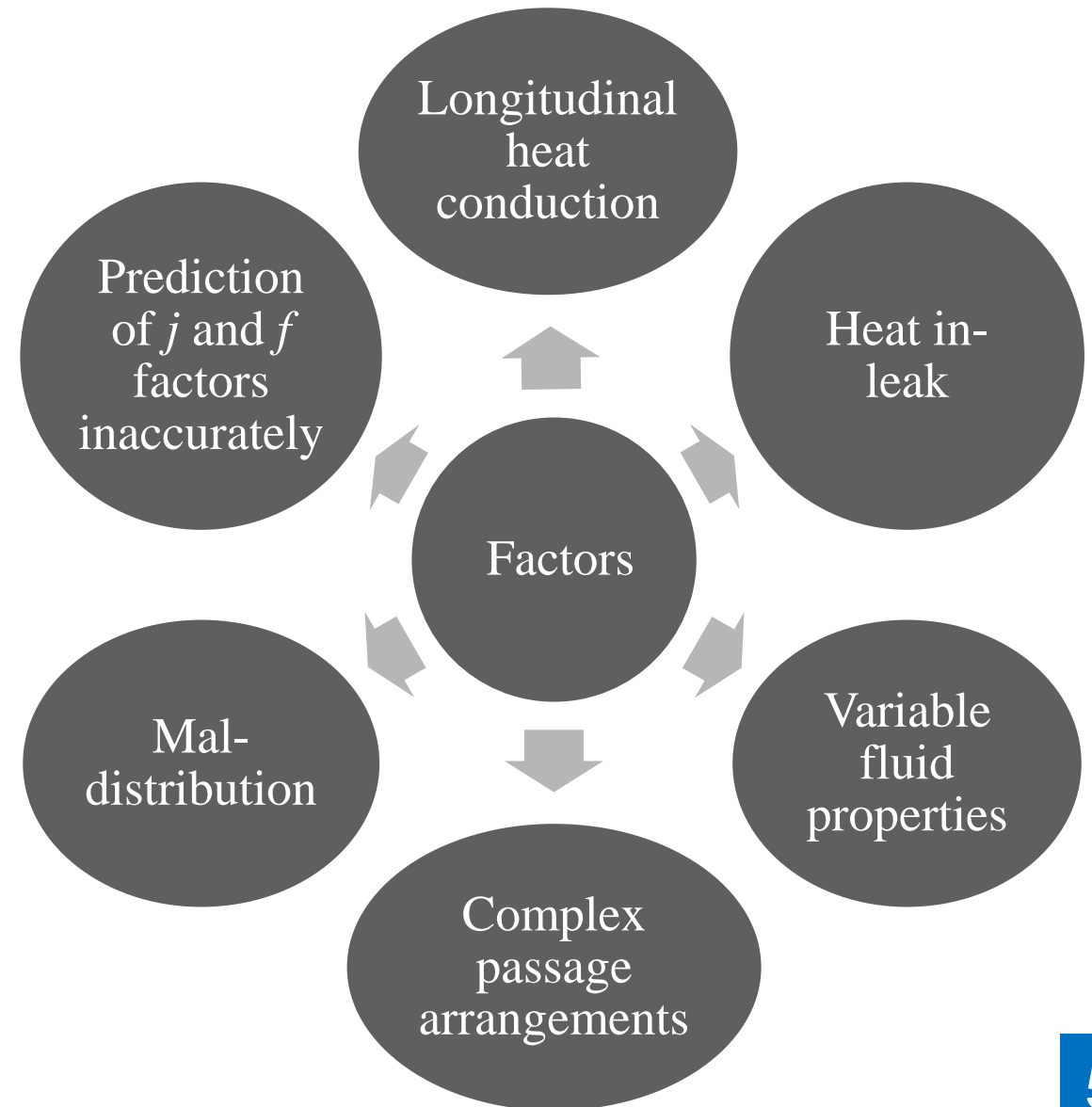
Table 2. Operation conditions

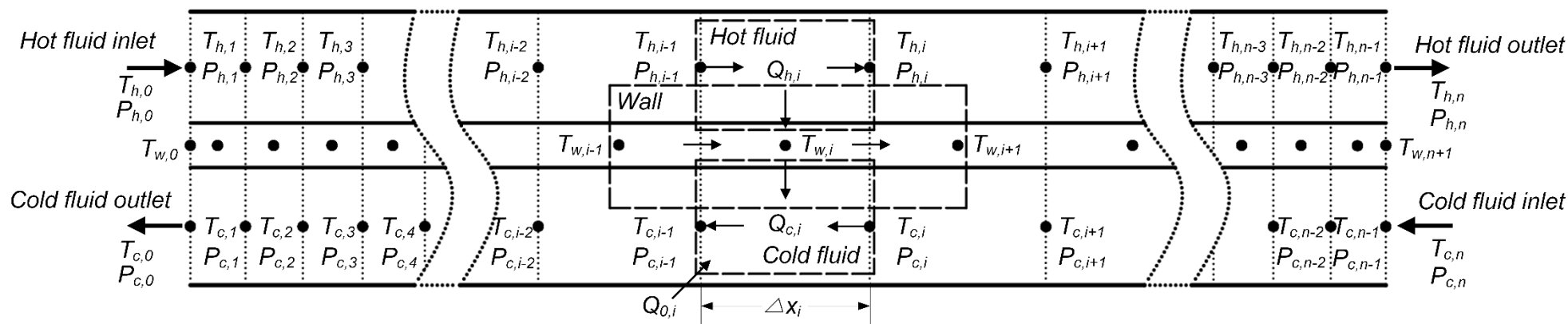
Stream number	Working fluid	Mass flow rate (gs ⁻¹)	Inlet temperature (K)	Inlet pressure (bar)	Number of layers	Layer pattern
A	Helium	59.2	300	19.5	22	A(BCA/4)D(BCA/4)D(BAC/4)D(ACB/4)D(ACB/4)A
B	Helium	41.3	77.8	1.1	20	
C	Helium	13.4	77.8	0.37	20	
D	Nitrogen	15.9	78.8	1.15	4	



The actual performance ?

Without considering manufacture errors, many additional questions may result in deviations from the original design condition:





A typical two-stream counter-flow recuperator

Hot fluid:

$$\left(\frac{v_{h,i} \Delta X_i}{v_{h,i-1} \Delta X_{i-1}} ntu_{h,i-1} + ntu_{h,i} \right) \left(\frac{\theta_{h,i} + \theta_{h,i-1}}{2} - \theta_{w,i} \right) + 2\alpha_{hi} NTU_i v_{h,i} \left(R - \frac{\theta_{h,i} + \theta_{h,i-1}}{2} + 1 \right) = \frac{\mu_{h,i} + \mu_{h,i-1}}{\mu_{h,i}} (\theta_{h,i-1} - \theta_{h,i})$$

Wall:

$$\begin{aligned} & \left(\frac{\Delta X_i}{v_{h,i-1} \Delta X_{i-1}} ntu_{h,i-1} + \frac{1}{v_{h,i}} ntu_{h,i} \right) \left(\frac{\theta_{h,i} + \theta_{h,i-1}}{2} - \theta_{w,i} \right) + 2 \frac{\lambda_{i-1} + \lambda_i}{\Delta X_{i-1} + \Delta X_i} (\theta_{w,i-1} - \theta_{w,i}) + 2\alpha_{wi} NTU_i \left(R - \frac{\theta_{w,i-1} + \theta_{w,i+1}}{2} + 1 \right) \\ & = \left(\frac{\Delta X_i}{v_{c,i-1} \Delta X_{i-1}} ntu_{c,i-1} + \frac{1}{v_{c,i}} ntu_{c,i} \right) \left(\theta_{w,i} - \frac{\theta_{c,i} + \theta_{c,i-1}}{2} \right) + 2 \frac{\lambda_i + \lambda_{i+1}}{\Delta X_i + \Delta X_{i+1}} (\theta_{w,i} - \theta_{w,i+1}) \end{aligned}$$

Cold fluid:

$$\left(\frac{v_{c,i} \Delta X_i}{v_{c,i-1} \Delta X_{i-1}} ntu_{c,i-1} + ntu_{c,i} \right) \left(\theta_{w,i} - \frac{\theta_{c,i} + \theta_{c,i-1}}{2} \right) + 2\alpha_{ci} NTU_i v_{c,i} \left(R - \frac{\theta_{c,i} + \theta_{c,i-1}}{2} + 1 \right) = \frac{\mu_{c,i} + \mu_{c,i-1}}{\mu_{c,i}} (\theta_{c,i-1} - \theta_{c,i})$$

$$\theta = \frac{T - T_{c,in}}{T_{h,in} - T_{c,in}} \quad \text{Dimensionless temperature}$$

$$R = \frac{T_a - T_{h,in}}{T_{h,in} - T_{c,in}} \quad \text{Dimensionless temperature gap}$$

$$\alpha_i = \frac{U_{o,i} A_{o,i}}{U_i A_i} \quad \text{Heat in-leak parameter}$$

$$\lambda_i = \frac{k_{w,i} A_c}{C_{min} L} \quad \text{Longitudinal conduction parameter}$$

$$v_{h,i} = \frac{C_{min}}{C_{h,i}} \quad v_{c,i} = \frac{C_{min}}{C_{c,i}} \quad \mu_{h,i} = \frac{C_{h,i}}{C_{h,in}} \quad \mu_{c,i} = \frac{C_{c,i}}{C_{c,in}} \quad ntu_{h,i} = \left(\frac{hA}{C}\right)_{h,i} \quad ntu_{c,i} = \left(\frac{hA}{C}\right)_{c,i} \quad NTU_i = \frac{U_i A_i}{C_{min}} \quad X_i = \frac{\Delta x_i}{L}$$

The core pressure drop in the i th section:

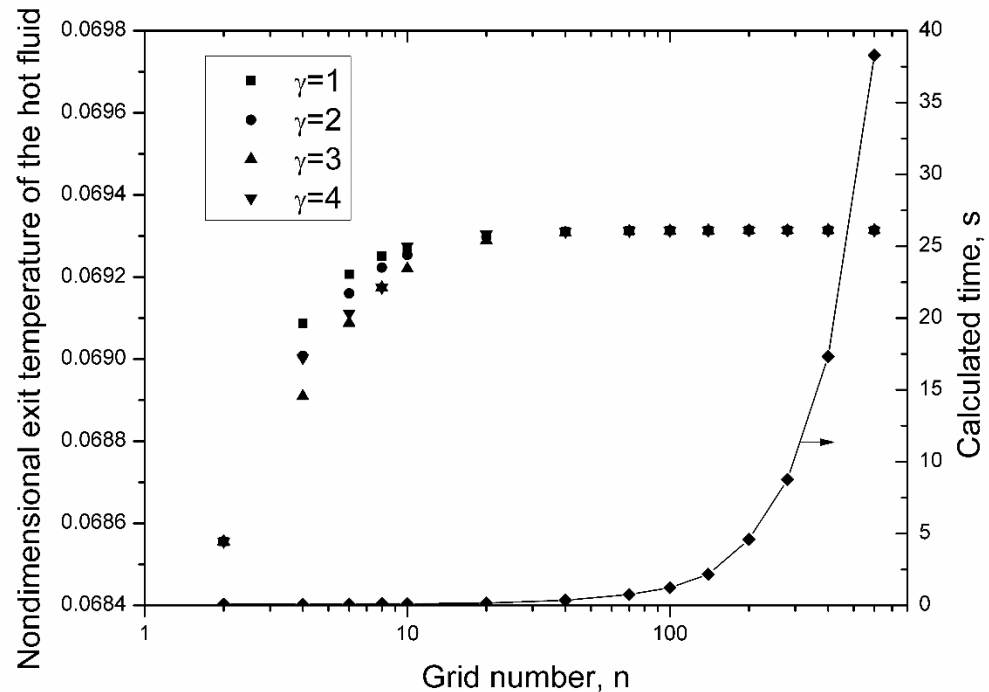
$$\Delta P_i = \frac{G^2}{2g_c} \left[\frac{4f}{D_h} \Delta x_i \left(\frac{1}{\rho}\right)_m + 2 \left(\frac{1}{\rho_{exit}} - \frac{1}{\rho_{entrance}} \right) \right]$$

Adiabatic ends for the wall:

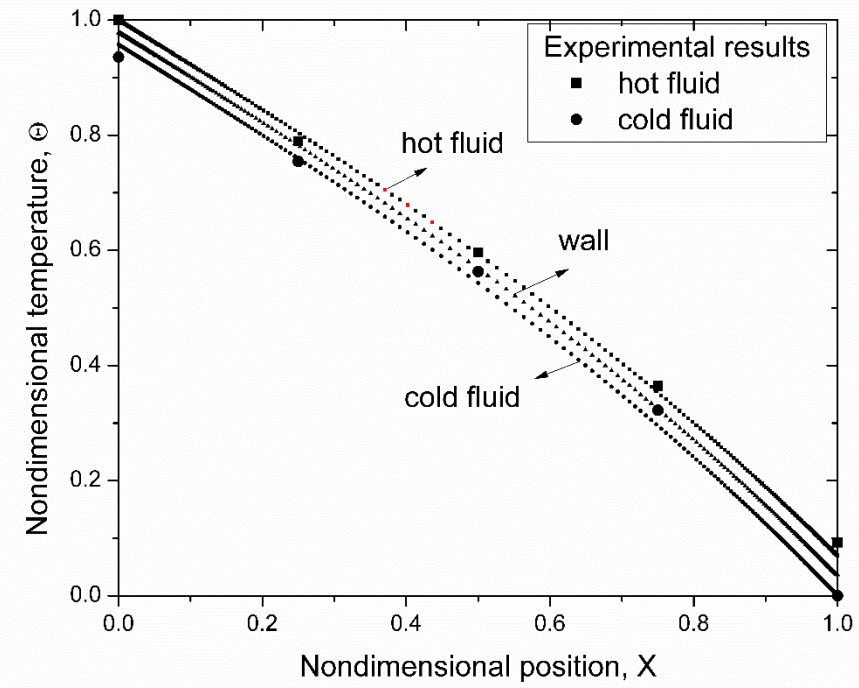
$$\theta_{h,0} = 1, \quad \theta_{w,0} = \theta_{w,1}$$

$$\theta_{c,n} = 0, \quad \theta_{w,n} = \theta_{w,n+1}$$

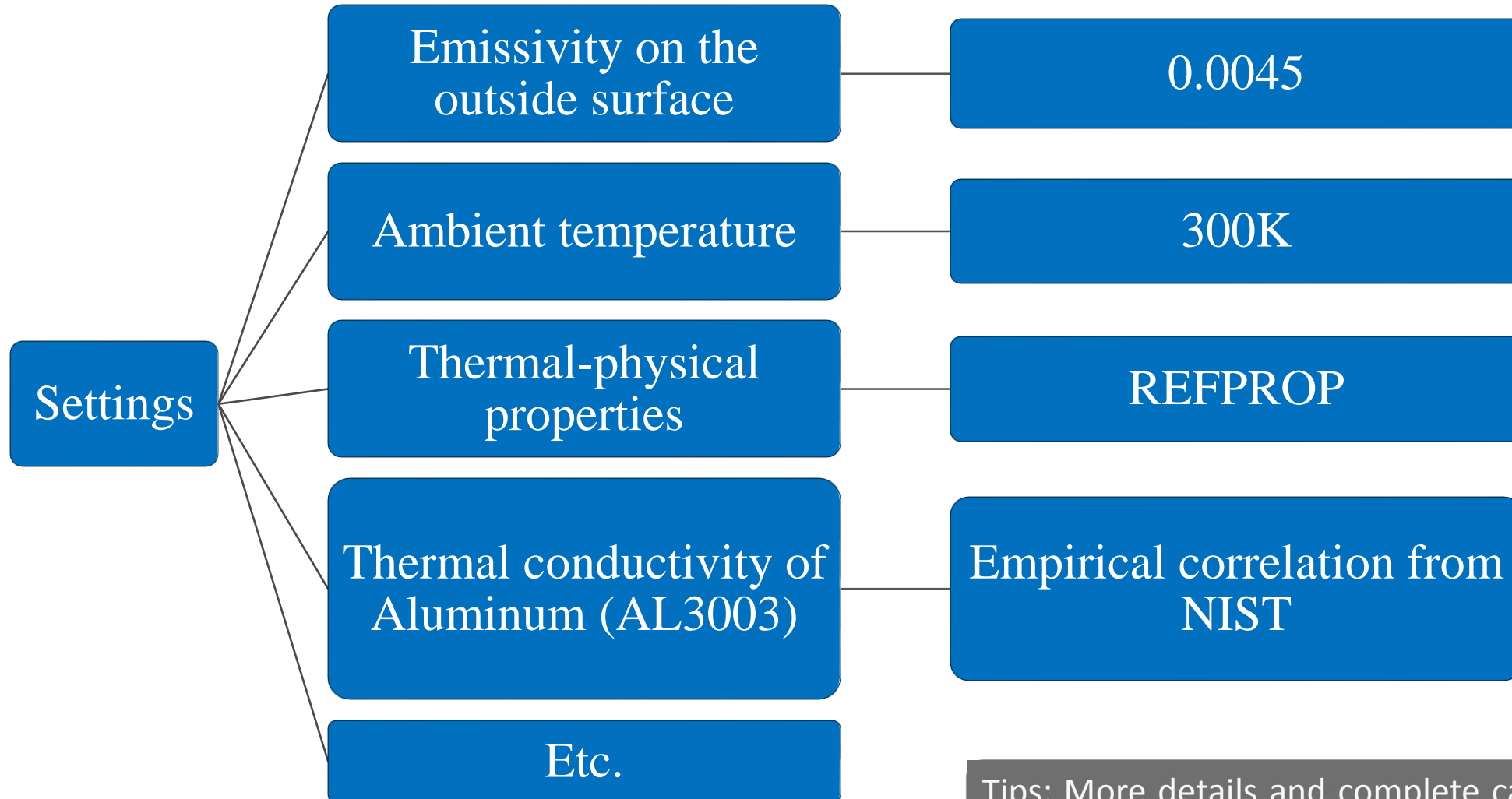
For the given cases about the coiled tube in tube heat exchangers



When $n = 100$, $\gamma = 4$, the precision and speed could be satisfied simultaneously



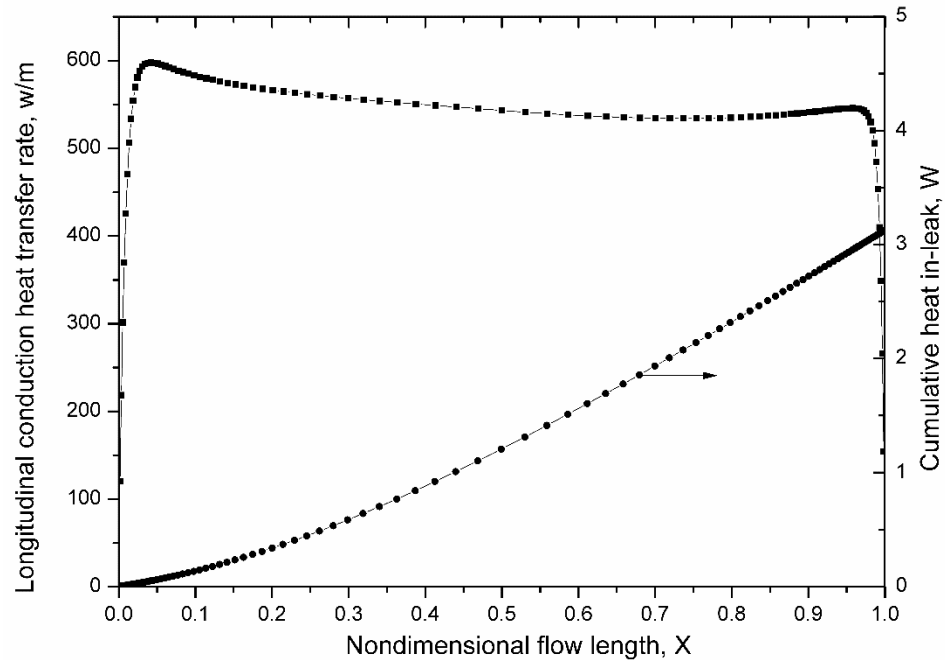
Prediction results assuming the constant fluid properties, empirical heat in-leak parameter and unchanged longitudinal conduction



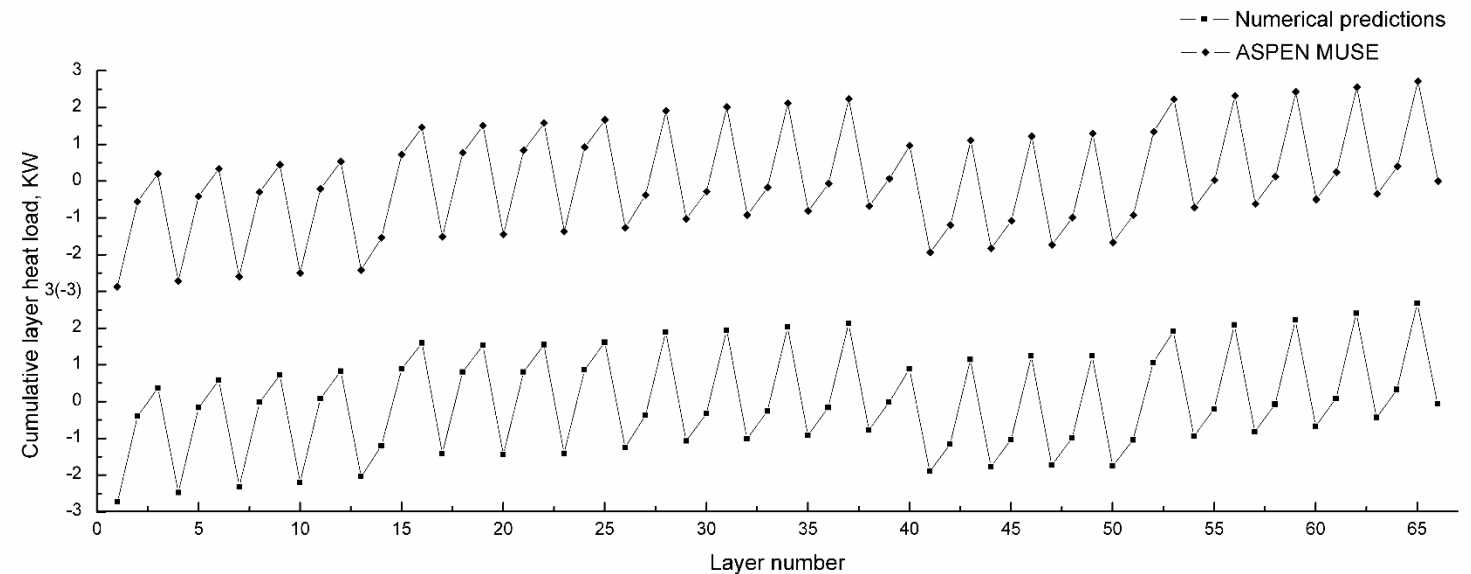
Tips: More details and complete calculation procedure can be found in the following submitted paper.

Table 3. Comparison results

Stream number	Outlet temperature (K)		Pressure drop (kPa)	
	MUSE	Numerical predictions	MUSE	Numerical predictions
A	90.26	92.60	0.15	0.18
B	291.81	289.37	0.88	1.09
C	292.28	291.38	0.64	0.81
D	290.94	286.71	0.24	0.29



Longitudinal conduction rate varies significantly and final cumulative heat in-leak reaches 3.12 W



Zig-zag chart about cumulative layer heat load



The numerical model taking into account of various loss mechanisms for counter-flow heat exchangers was investigated.

1. Different from the previous lumped parameter models, the model based on distributed parameter methods could calculate the performance, evaluate longitudinal wall conduction and predict heat in-leak in each finite section.
2. Great deviations from the original design condition might be caused by various losses occurred in the actual operating environment.
3. The method could be useful to evaluate and rate the heat exchanger performance under the actual cryogenic conditions.



Thanks for listening !
